Dynamical Climatology

Atmospheric general circulation model simulation of the climate of the Mediterranean region

by

H. Cattle

DCTN 17 February 1985

Meteorological Office (Met. O. 20)
London Road
Bracknell
Berkshire RG12 2SZ

DYNAMICAL CLIMATOLOGY TECHNICAL NOTE NO. 17

ATMOSPHERIC GENERAL CIRCULATION MODEL SIMULATION OF THE CLIMATE OF THE MEDITERRANEAN REGION

by

H. Cattle

This paper was presented at the NATO Workshop on Atmospheric and Oceanic Circulation in the Mediterranean Basin, Lerici, Italy, 7-14 September 1983.

Met O 20 (Dynamical
Climatology Branch)
Meteorological Office
London Road
Bracknell
Berkshire, U.K. RG12 2SZ

February 1985

Note: This paper has not been published. Permission to quote from it should be obtained from the Assistant Director of the above Meteorological Office Branch.

Atmospheric General Circulation Model Simulation of the Climate of the Mediterranean Region

By Howard Cattle

Dynamical Climatology Branch, Meteorological Office, Bracknell UK

Introduction

The climate of a region can, in many ways, be regarded as the statistical description of its weather. In being asked to discuss the way in which the Mediterranean climate is simulated by atmospheric general circulation models (AGCMs) the question therefore naturally arose as to how the large scale nature (in a spatial sense) of such modelling would match the requirements for representing the climate of a region for which the detailed topography is so important for the weather systems which are found there and which, furthermore, are often of such a scale as to be inadequately resolved by the GCM grid. An adequate description of the local climate by such a model depends, of course, not only on the representation of smaller scale features but also upon an adequate simulation of the large (continental) scale systems and their evolution through the annual cycle. Atmospheric general circulation climate models are not, of course, necessarily intended for detailed regional scale studies but rather for the study of the global circulation of the atmosphere as a whole, both in the context of attempting to simulate and gain insight into the world climate and its variability as well as to understand the response of the atmosphere to variations in the large scale forcing (sea surface temperature anomalies, for example) and the atmospheric composition (carbon dioxide, ozone, dust concentrations etc).

Such models are restricted, to a large extent, in their resolution, by the available computing power so that the grid they employ is often relatively coarse for regional scale studies. The results described here are largely drawn from an eight year annual cycle integration of the Meteorological Office 11 layer AGCM on a 2.5° x 3.75° latitude longitude grid which gives a resolution over the Mediterranean region of some 280 x 340 km. Figure 1 shows a section of the horizontal grid of this model over an area centred on the Mediterranean and covering much of the North Atlantic, Europe and North Africa. A grid point is classified as either

land or sea according to whichever is in the greater proportion over the corresponding grid square as determined objectively from a fine mesh (1° x 1°) dataset of the land/sea distribution over the globe. Note the highly simplified nature of the coastline. Both this and the grid resolution are typical of such models.

As already mentioned, the topography of the Mediterranean region is an important factor for its weather and climate (see e.g. Meteorological Office, 1962). Except along the North African coast east of Tunisia, the sea is enclosed by mountain ranges which run down close to the coastline which itself is highly indented. A variety of local effects therefore present themselves: anabatic, katabatic and ravine winds, land and sea breezes, local strengthening of the wind by horizontal confluence, eddying, particularly to the lee of steep topography, and so on. Such effects will not be represented by the GCM. The mountain ranges present substantial barriers to the flow of air into the Mediterranean, with the air forced to rise over or circumvent them. Many of the depressions which form in the Mediterranean in winter are the result of lee cyclogenesis, particularly to the south of the Alps, whilst much of the air which flows into the Mediterranean region arrives through gaps in the mountain ranges with which a number of well known regional winds are associated. Important amongst these are the northwesterly Mistral, which flows through the Alps -Pyrenees gap; the northeasterly Bora, which flows through the Trieste gap; the easterly Levander and westerly Vendaval, which flow through the Straits of Gibraltar; the winds which enter the Mediterranean via the low land to the north and northeast of the Aegean Sea (Bora type winds in winter and the Etesian winds of summer) and the broader flow of warm southerly winds which sometimes enter the region from the flatter southern shores of North Africa (Scirocco). Figure 2 shows the orography of the numerical model around the peripheries of the Mediterranean. It, too, is highly smoothed compared with reality but indicates that the numerical model can attempt to simulate the barrier effects of the mountains including the passage of air into the Mediterranean via the lower ground between them.

General circulation models attempt, of course, to take into account most of the features important for climate, including representation of radiative and boundary layer fluxes and rainfall associated with convective and large scale disturbances. The Meteorological Office 11 layer AGCM is a

global model, a version of which, described by Lyne and Rowntree (1983), was developed for the GARP tropical experiment. It is a primitive equation grid point model using sigma (σ) coordinates (σ = the ratio of pressure at any level to the surface pressure) in the vertical. Use of such a coordinate system allows a more satisfactory description of the flow around topography than does, for example, use of pressure itself as a vertical coordinate. Surface pressure is predicted at each grid point and values of temperature, horizontal wind components and specific humidity are predicted at each grid point at each level. The seasonal and diurnal variation of solar radiation are both represented and the radiative fluxes expressed as a function of temperature and water vapour, carbon dioxide and ozone concentrations and prescribed zonal mean cloudiness. Versions of the model in which the cloudiness is determined within the model itself are currently under test. The seasonal cycle of sea surface temperatures and ice extents is prescribed from climatology, and is updated every 5 days of model time. The model also incorporates a penetrative convection scheme which can operate throughout the troposphere. For the simulations described below, a stability dependent boundary layer scheme based on Clarke (1970) was used. This operates over the three lowest layers of the model (up to about 800 mb over the sea) where the vertical resolution is highest. The equations were integrated forward in time with a timestep of 10 minutes over some 8 annual cycles on the Meteorological Office's Cyber 205 computer for which the CPU time averaged some 3 minutes per day. Initial data were taken from a FGGE analysis for 25 July 1979.

Simulations of the winter climatology

The mean sea level pressure distribution in January In a broad sense the climate of the Mediterranean possesses the marked seasonal characteristics of windy, mild, wet winters and hot dry summers. These seasonal features are linked to the evolution through the year of the large scale pressure systems over the Atlantic, Eurasia and Africa. Figure 3a shows the observed mean sea level pressure distribution for January taken from the climatological dataset of Schutz and Gates (1971). Note in particular the central pressures and positions of the low pressure over the North Atlantic (the Icelandic low, central pressure 998 mb) and of the Azores (central

pressure 1024 mb) and Siberian (central pressure 1026 mb) highs, decreasing pressure over North Africa towards the equatorial trough and the strengths of the mid latitude westerlies as implied by the horizontal pressure gradient between the Azores high and Icelandic low pressure systems. There is relatively low pressure over the Mediterranean itself where the mean pressure gradients are quite slack.

Figure 3b shows the monthly mean sea level pressure distribution from the second January (picked at random) of the model integration. The same contour interval of 2.5 mb has been employed as for Figure 3a. The model simulation shows mid latitude westerlies which are much stronger than observed with low pressure to the north which is too deep and the centre of which is positioned to the north of Scandinavia, with a trough extending southwestwards towards Iceland. The position of this low pressure system represents something of an extreme for the model simulation. In other years it is found somewhat further towards (but not over) its observed position. The Siberian high is weaker than observed whilst the Azores high is more intense and centred just to the west of the Iberian Peninsula at about 12°W rather than off the Straits of Gibraltar at around 20°W (cf Figure 3a). Over the Mediterranean, low pressure predominates in the extreme east of the area, centred over Cyprus, with a marked east-west gradient over much of the remainder of the Mediterranean Sea. This is in contrast to the rather slack area of low pressure which we have seen to predominate on the climatological chart. Note some evidence of troughing, however, in the northerly flow. To the south of the Mediterranean, the pressure in the equatorial trough is just about right.

It must be remembered that we are, of course, comparing a particular model January with a 30 year climatological mean. Just as an individual observed January mean will differ from the 30 year mean within the natural variability of the atmosphere, so this January mean differs from the corresponding climatological mean of the model. The model possesses its own climatic variability, consistent with the constraint that the seasonal variation of sea surface temperatures and sea ice is prescribed and constant from year to year. Some indication of the model variability for the Mediterranean and surrounding areas in winter can be obtained from Figure 4 which shows the average mean sea level pressure for the first, third, fourth and fifth Januaries of the model integration. There is, in

fact, a notable variation from one year to the next, though most of the features commented on above show through. The third January of the run is the most like that of the observed long term mean. It is evident, however, that there is substantial misrepresentation of a number of the major features of the January circulation which affects the detailed simulation by the model of the climate of the Mediterranean Basin itself. Figure 5 shows January simulations by models from three other Centres, namely the NCAR, GFDL and OSU AGCMs. The contour interval here is twice that used previously, namely 5 mb. These models show errors which are different, but comparable in magnitude to those for the Meteorological Office model. Thus both the NCAR and OSU models show the belt of mid latitude westerlies to be too far south. The GFDL model is somewhat better, though the westerlies penetrate too far southeastwards into Europe, giving a marked west to northwest flow over much of the northern Mediterranean. Note the presence of a surface trough over the Mediterranean in both the NCAR and GFDL models, indicative of the role of the Sea as a heat source in winter (see also Figure 4).

The upper flow over the Mediterranean in winter (January) Figure 6a shows a Meteorological Office analysis (Benwell, 1982) of the climatological mean 500 mb geopotential field over the Mediterranean region for January. A notable feature is the European mid tropospheric trough which is of particular relevance for the weather of the region during the winter months. It extends from Novaya Zemlya southwards over the central Mediterranean and into North Africa. In fact the southernmost position of the trough is highly variable, both on a month to month and year to year basis. It may be found over a range of longitudes ranging from 10°W to 30°E and its location has been used to classify the character of the weather over the Mediterranean region. (See eg. Boucher 1975). The model simulation puts the trough too far east. Figure 6b is typical and shows the trough extending southwestwards into the Mediterranean from the central Black Sea and then westwards across North Africa. The model also has it varying from year to year more in amplitude than position, in association with the strength of the ridge over the North Atlantic which Figure 6b shows to extend over the Iberian Peninsula from the area west of the Canary Islands. The model gradients in this region are generally much slacker than

in nature whilst, as noted earlier for the surface pressure field, the midlatitude westerlies to the north are much too strong. Figure 7 compares the observed, seasonally averaged, winds for December, January and February at 400 mb given by Schutz and Gates (1973) with the 450 mb model fields for the corresponding months for the second winter of the run. Note the weak meridional flow (which sometimes has an easterly component) over the Atlantic west of Gibraltar in the model with the winds becoming more westerly and stronger towards the eastern end of the Mediterranean. The observed flow has similar characteristics but is stronger and more uniform with a transition from flow from the west north west over the western Mediterranean to almost westerly in the east of the region, where merging of the subtropical and polar front jetstreams is a not infrequent occurrence (Wigley and Farmer, 1982). Much of the variability in the model winds at these levels is associated with the amplification and relaxation of the ridge-trough system mentioned previously. In the former case the model winds over the central Mediterranean become stronger and more northerly whilst a relaxation of the trough/ridge system with accompanying strengthening of the westerly gradient can lead to winds more from the west-northwest over much of the region.

The distinction between the flow in the polar front and subtropical jets over the Mediterranean is more apparent in the model at 450 mb than in the observations at 400 mb. Figure 8 compares the observed cross section of mean wind speed at 15°E for January (taken from Meteorological Office, 1962) with a corresponding cross section of the zonal component of the wind from the model at 17°E, again for the second January of the integration. The speed and level of the flow in the subtropical jet are both well represented by the model, if a little too far south whilst the flow of the mid latitude westerlies is, as remarked earlier, rather too strong.

The simulation of the summer climatology

The mean sea level pressure field in July As noted previously the Mediterranean region has markedly different summer and winter regimes. The transition from summer to winter is usually fairly decisive with winter patterns setting in during October, whilst the transition from winter to summer takes place in a number of 'false starts'. Figure 9a shows the

characteristic summer surface pressure field, illustrated by the climatological mean for July. Notable features in the development of the large scale circulation systems which lead to the establishment of this pattern are the collapse of the Siberian anticyclone during spring, the extension of the Azores high over the Mediterranean and the development of the Asian monsoon low which itself extends westwards towards the Mediterranean across Asia Minor resulting in a trough which cuts across Turkey and into Greece. Note the ridge which extends northeastwards across Central Europe from the Azores high with another extending southeastwards towards Egypt. These developments usually begin during April with summer conditions becoming well established over the Mediterranean by June (Meteorological Office 1962).

Whilst the details of the transition from winter to summer conditions are not particularly well represented by the model (not shown), the surface pressure pattern which is established by July (Figure 9b) compares quite well with that observed. The model slowly lost mass as the integration proceeded due to roundoff errors in the computation (a problem which has since been solved). To correct for this, the surface pressure was uniformly adjusted over the entire grid at the end of each model year from the second onwards. As a result however the surface pressures in the model are too low by some 6 mb in the second July so that the values in Figure 9b should be increased by this amount everywhere which brings them closer to the climatological levels. Figure 9b is, in fact, characteristic of the July simulation for each year of the model run. The simulation shows the Atlantic high to be too far to the northeast resulting in a ridge over the southern United Kingdom and northern Europe which is rather too intense. Gradients are too slack in the region of the northeast trades but too steep on the seaward side of the Atlas mountains. Nevertheless the character of the surface pressure field over the Mediterranean is, as remarked above, quite faithfully reproduced.

The upper flow during summer (July) Whilst the surface pressure field in summer is well represented, this is less true for the flow in the upper atmosphere. At 500 mb (Figure 10b is typical) the model shows gradients which are too slack over the Mediterranean compared with climatology (Figure 10a), with stronger westerlies over northern Europe which do not

extend far enough south. The ridge-trough pattern in the flow near 450 mb (Figure 11) over the Mediterranean is present in the model simulation though in general speeds are too low over the Mediterranean and too strong over North Africa. Figure 12 compares the observed and modelled wind cross sections at 15 and 17°E respectively. The subtropical jet shifts northward during March to May to a position on the northern side of the Mediterranean with weaker flow in the mid latitude westerlies further north. This is indicated to some extent in the model cross section though, as noted above in relation to Figure 11, the westerly flow in middle levels to the south remains too strong. The upper level easterlies are also too intense.

The annual cycle of rainfall over the Mediterranean

It is well known that during the winter months the Mediterranean forms one of the world's major centres of cyclogenesis (see eg. Pettersen, 1956). The low pressure centres themselves tend to be rather shallow when compared to their counterparts in the Northern Atlantic. Indeed the latter rarely penetrate into the Mediterranean, whilst the Mediterranean lows themselves are often related to much larger disturbances north of the Alps. From this point of view they can be considered as secondary depressions (Boucher, 1975) and as such are relatively small scale. In consequence they are not well resolved by the 2.5° x 3.75° grid of the numerical model. As a result of the cyclonic activity, rainfall over the Mediterranean is at its maximum during the winter months but gives way to dry conditions during the summer months when the Mediterranean lies more under the influence of the subtropical high pressure regime. The seasonal transition in the rainfall pattern is illustrated by Figure 13, taken from Schutz and Gates' (1971,2,3,4) tabulation of Moller's (1951) rainfall analysis. This shows precipitation values of order 2 mm day^{-1} over the Mediterranean during the winter months (December to February) with a marked gradient across the coast of North Africa to the desert conditions of the Sahara. The pattern shifts northward during the spring and early summer to bring the gradient in the isohyets to the north of the Mediterranean during the summer months (June to August). By autumn (October to November) the pattern has shifted back southwards as the cyclonic winter regime sets in.

Whilst the model grid resolution is not such as to allow an adequate detailed representation of Mediterranean depressions, nevertheless the characteristics of the seasonal evolution of the rainfall pattern of the region are quite well simulated by the model. This is because the Mediterranean acts as a source of sensible heat during winter (see below) which, coupled with its role as a moisture source, acts as a trigger to the model's convective rainfall scheme. Indeed very little of the model rainfall over the Mediterranean (less than 0.5 mm day^{-1} during winter) results from the condensation on the grid scale. Most is produced as a result of the operation of the convective scheme, in contrast to the situation, for example, over northern Europe during the winter months. This is illustrated by Figures 14 and 15 which show the rainfall rates for modelled dynamical and convective rainfall respectively and which can be compared directly to Figure 13 (the total model rainfall rate is, of course, given by the sum of the values given in Figures 14 and 15). Note the maximum in the convective rainfall over the Mediterranean in winter (of order 2 to 4 mm day^{-1}) with peak values then over the eastern basin in association with the centre of low pressure there (cf Figure 3b). Dry conditions prevail in the model over much of the Mediterranean during the spring and summer months with the convective rainfall setting in again during the autumn, though anomalous maxima are found over the high ground over central Spain and to the east of the Atlas mountains during June to August.

Heat and moisture fluxes from the sea surface

As remarked above, the Mediterranean acts as a substantial source of sensible heat during the winter months when sea surface temperatures are 1 to 2C warmer than the air in the south and west of the region and some 3 to 4C warmer in the north and east. In summer the sign of the temperature difference is reversed and typically of magnitude 0.5 to 1C (see for example the analyses of Repapis, Metaxis and Zerefos, 1978). Larger differences may, of course, occur in particular synoptic situations. Thus Bunker (1972) observed air-sea temperature differences of 8C and more during an occasion of well developed Mistral flow over the Gulf of Lions. Figure 16 compares the sensible heat exchange over the Mediterranean as derived climatologically from data by Repapis, Metaxis and Zerefos (1978)

with model values. Note the marked contrast in the model fields between sea and land, over which stable conditions predominate. Over the Mediterranean Sea itself there is a marked southwest to northeast gradient in the sensible heat flux both as derived from observations and as simulated, with model values attaining a maximum of some 230 cal cm^{-2} day^{-1} (110 Wm^{-2}), about twice that of the climatologically observed figure. This discrepancy is not surprising in view of the differences between modelled and observed flows and in the algorithms used to derive the fluxes. The fields of climatological and simulated fluxes should be viewed against the particular land/sea configurations and the orographic features to which they refer. Note that in the model the maxima occur essentially on the leeward side of the gaps in the mountain ranges along the northern coast (cf Figure 3b). In summer, when the air-sea temperature difference is small, the heat flux is directed into the surface over much of the Mediterranean Sea. Its size then is typically of order 10 cal cm^2 day^{-1} (5 Wm^{-2}) with maxima of some 30 cal cm^{-2} day^{-1} (15 Wm^{-2}) close to the coast in the Gulf of Lions and 50 cal cm^{-2} day^{-1} (25 Wm^{-2}) off the Turkish coast of the Aegean Sea (see, for example Repapis, Metaxis and Zerefos, 1978). Model values (not shown) are comparable and again directed into the surface.

The Mediterranean acts as a source of moisture for the atmosphere throughout the year. Indeed evaporation exceeds precipitation and run off so that the water loss must be balanced by a net inflow of (relatively fresh) water from the Atlantic. Evaporation is greatest from about September to January when average values of about 6.5 mm day^{-1} are found for the Mediterranean east of 20°E and 5 to6 mm day^{-1} west of 20°E (Metaxis and Repapis (1977)) though see also Colacino and Dell'Osso (1977) who show rather lower values for the western and central Mediterranean). Model values compare quite favourably. Figure 16 show the January fields derived by Metaxis and Repapis against the evaporation rates found in the model, the latter being characteristic of those observed. Typically they are between 4 and 7 mm day^{-1}, with maximum values at this time of year in much the same locations as for the sensible heat flux.

Concluding remarks

It is evident that errors in the AGCM simulations of large scale features of the general circulation are such as to markedly affect the way in which such models represent the Mediterranean climate. Further, different models have different errors which will influence the simulated climate of the region in different ways. Nevertheless from the results discussed here for the Meteorological Office model it is evident that certain broad features of the Mediterranean climate can be identified in the simulation. In particular the marked transition from winter to summer conditions is represented, as reflected by the characteristics of the modelled mean sea level pressure fields, seasonal shift in the upper level jet and (convective) precipitation patterns. There is also some evidence for the wintertime role of the Mediterranean as a heat source, indicated by the presence of a wintertime trough superimposed on the large scale surface pressure field. Further, though the wintertime sensible heat exchange may be overestimated, model values both for this and the evaporative flux over the Mediterranean are not necessarily unrealistic, whilst the seasonal variation of the fields of these parameters is also quite well represented by the model.

References

Benwell, P.R., 1982. Standard contour datasets. London, Meteorological Office. Met O 13 Data Processing Section Technical Note No. 7 (unpublished, copy available in the National Meteorological Library, Bracknell).

Boucher, K., 1975 Global climate, English Universities Press.

Bunker, A.F., 1972 Wintertime interactions of the atmosphere with the Mediterranean Sea. J Phys Oceanogr. 2 pp 225-238.

Clarke, R.H., 1970. Observational studies in the atmospheric boundary layer. Quart. J.R. Met. Soc. 96 pp 91-114.

Colacino, M. and L. Dell'Osso, 1977. Monthly mean evaporation over the Mediterranean Sea. Arch. Met. Geoph. Biokl., Ser. A, 26 pp 283-293.

Lyne, W.H., and P. R. Rowntree, 1983. Forecast model. In: The Meteorological Office GATE modelling experiment, edited by P R Rowntree and H Cattle, Meteorological Office Scientific Paper No. 40, pp 34-40.

Manabe, S., Hahn, D.G., and J.L. Holloway Jr., 1979. Climate simulations with GFDL spectral models of the atmosphere: effect of spectral truncation. In Report of the JOC study conference on climate models: performance, intercomparison and sensitivity studies. Volume 1, edited by W L Gates. ICSU/WMO GARP publications series No 22 pp 41-94.

Metaxis, D.A., and C.C. Repapis, 1977. Evaporation in the Mediterranean. Rivista Di Meteorologia Aeronautica - V.XXXVII pp 311-317.

Meteorological Office, 1962. Weather in the Mediterranean Vol. 1. Her Majesty's Stationary Office, London.

Pettersen, S., 1956. Weather analysis and forecasting (second edition). Vol. 1. McGraw Hill, New York.

Repapis, C.C., Metaxis, D.A., and C.S. Zerefos, 1978. Spatial and seasonal climatology of sensible heat flux over the Mediterranean Sea. Research Center for Atmospheric Physics and Climatology, Academy of Athens, Greece. Technical Report No. 138.

Schlesinger, M.E., and W.L. Gates., 1979. Performance of the Oregon State University two-level atmospheric general circulation model. In Report of the JOC study conference on climate models: performance, intercomparison and sensitivity studies. Volume 1, edited by W L Gates. ICSU/WMO GARP publications series No. 22, pp 139-206.

Schutz, C. and W.L. Gates, 1971. Global climatic data for surface, 800 mb, 400 mb: January. The Rand Corporation R-915-ARPA.

_____ 1972. Global climatic data for surface, 800 mb, 400 mb: July. The Rand Corporation, R-1089-ARPA.

_____ 1973. global climatic data for surface, 800 mb, 400 mb: April. The Rand Corporation. R-1317-ARPA.

_____ 1974. GLobal climatic data for surface, 800 mb, 400 mb: October. The Rand Corporation, R-1425-ARPA.

Washington, W.M., Dickinson, R., Ramanathan, V., Mayer, T., Williamson, D., Williamson, G., and R Wolski, 1979. Preliminary atmospheric simulation with the third generation NCAR general circulation model: January and July. In Report of the JOC study conference on climate models: performance, intercomparison and sensitivity studies. Volume 1, edited by W. L. Gates. ICSU/WMO GARP publications series No. 22, pp 95-138.

Wigley, T.M.L. and G. Farmer, 1982. Climate of the eastern Mediterranean and Near East. In. Paleoclimate, paleoenvironments and human communities in the eastern Mediterranean region in later prehistory, edited by J.L. Bintliff and W Van Zeist. Brit. Archaeol. Rep. BAR Int. Ser. 133(i), Oxford. pp 3-37.

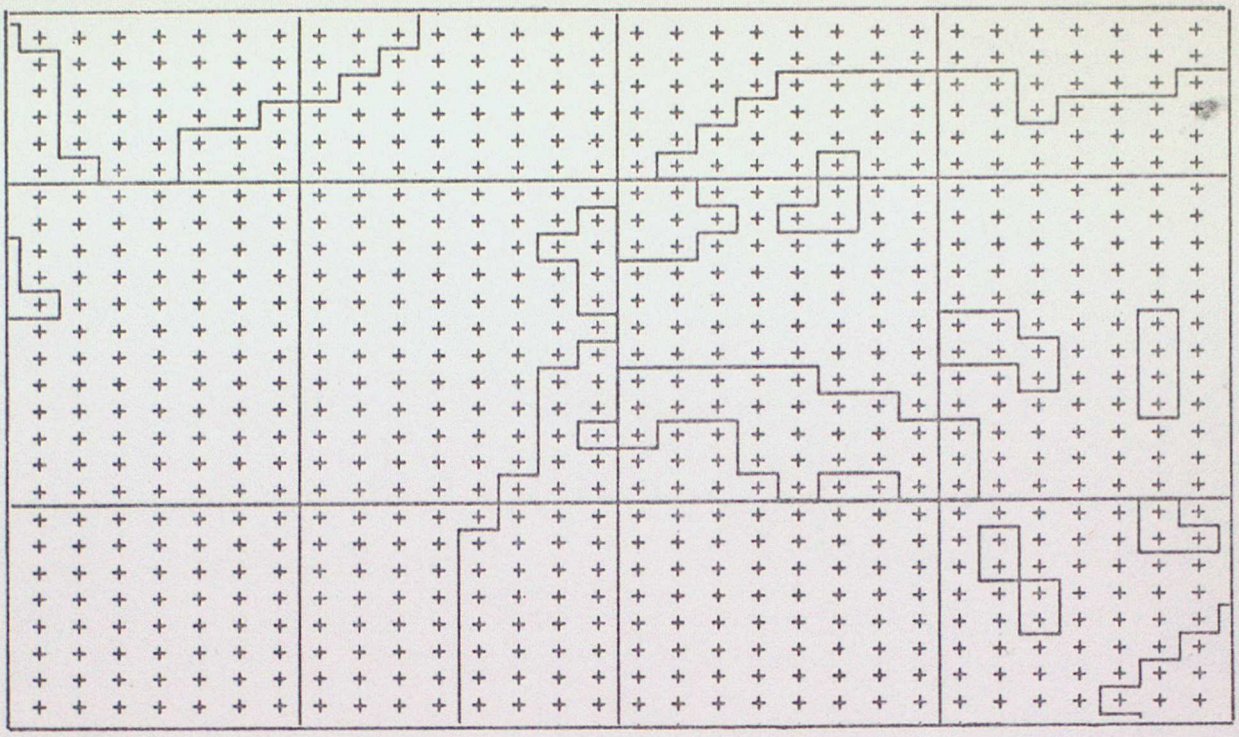

Figure 1 Section of the horizontal grid of the Meteorological Office 11 layer atmospheric general circulation model covering the region of the North Atlantic, Europe and North Africa. The model coastline is also marked.

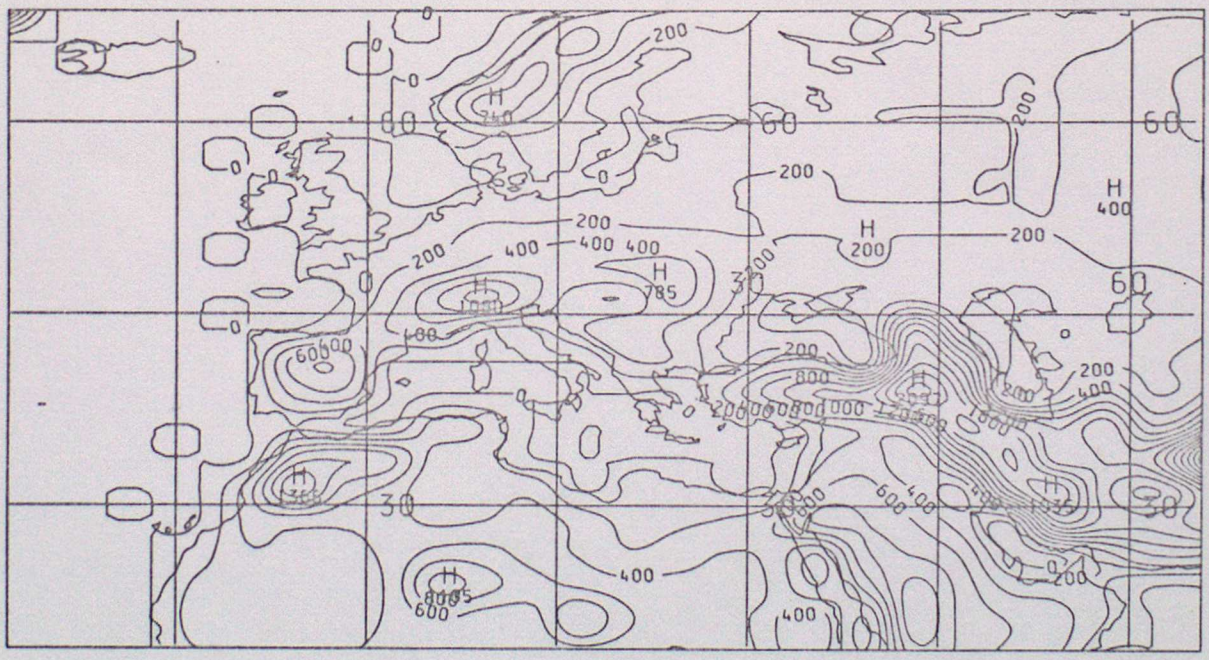

Figure 2 Orography of the numerical model around the peripheries of the Mediterranean Sea. Contours are drawn at intervals of 200 gpm.

(a)

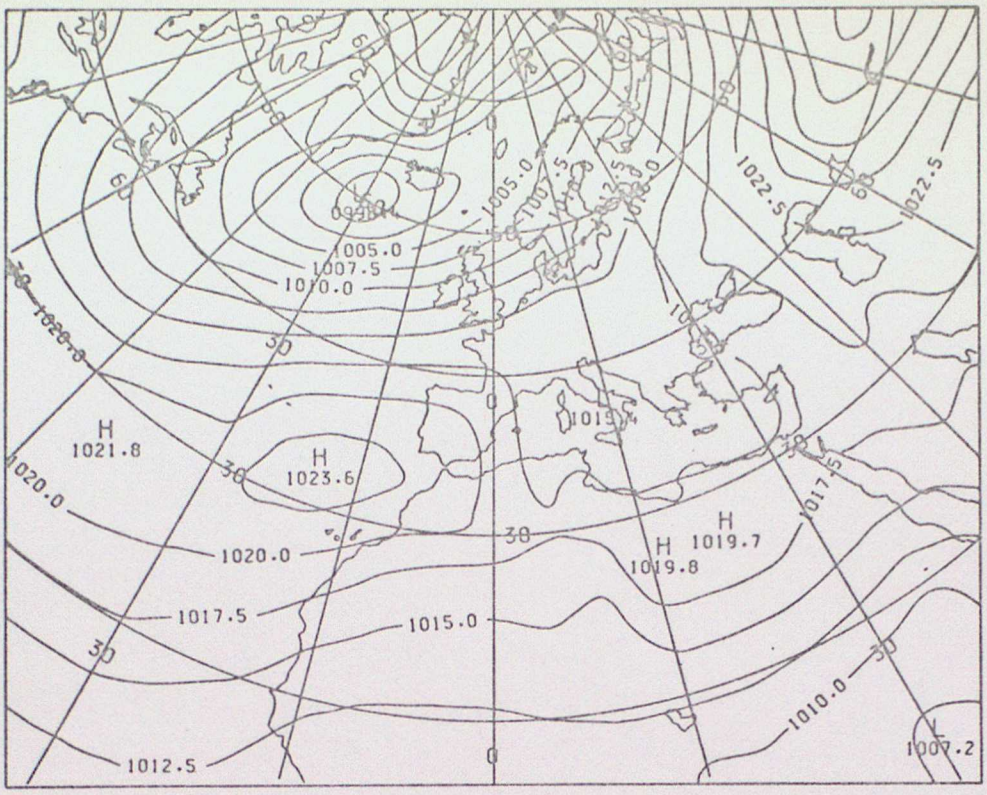

(b)

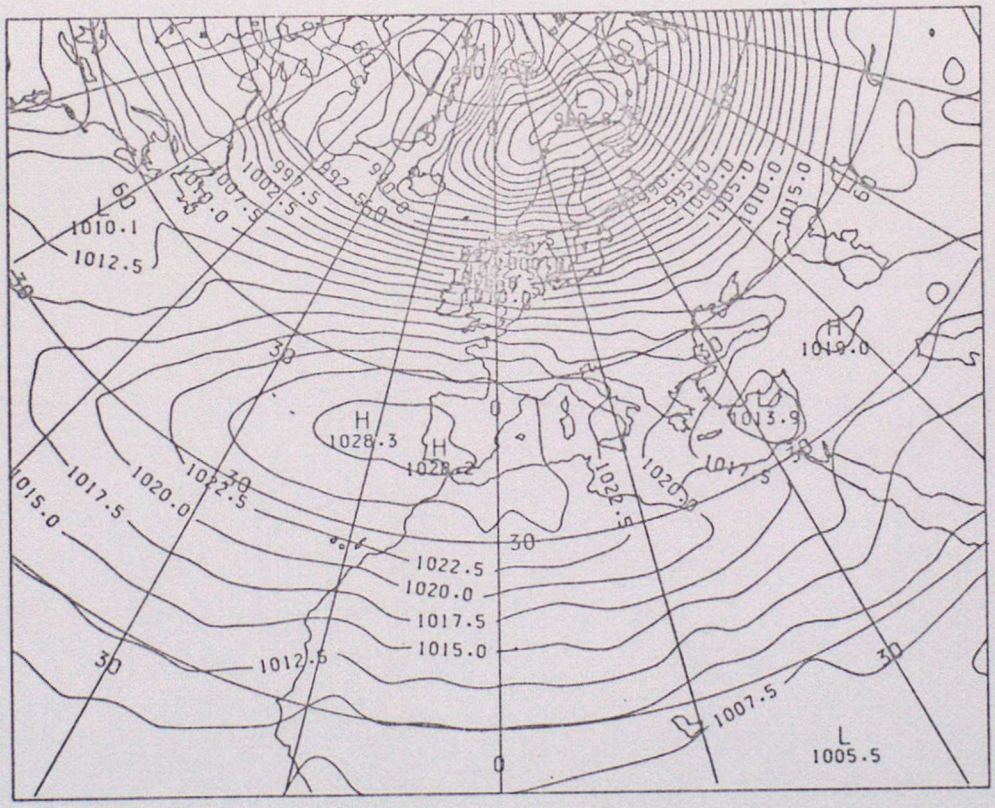

Figure 3 Comparison of (a) the observed climatological mean sea level pressure distribution for January for the Mediterranean and surrounding region (from Schutz and Gates, 1971) with (b) the model mean sea level pressure distribution for the second January of the multiannual cycle integration. Contours are drawn at 2.5 mb intervals.

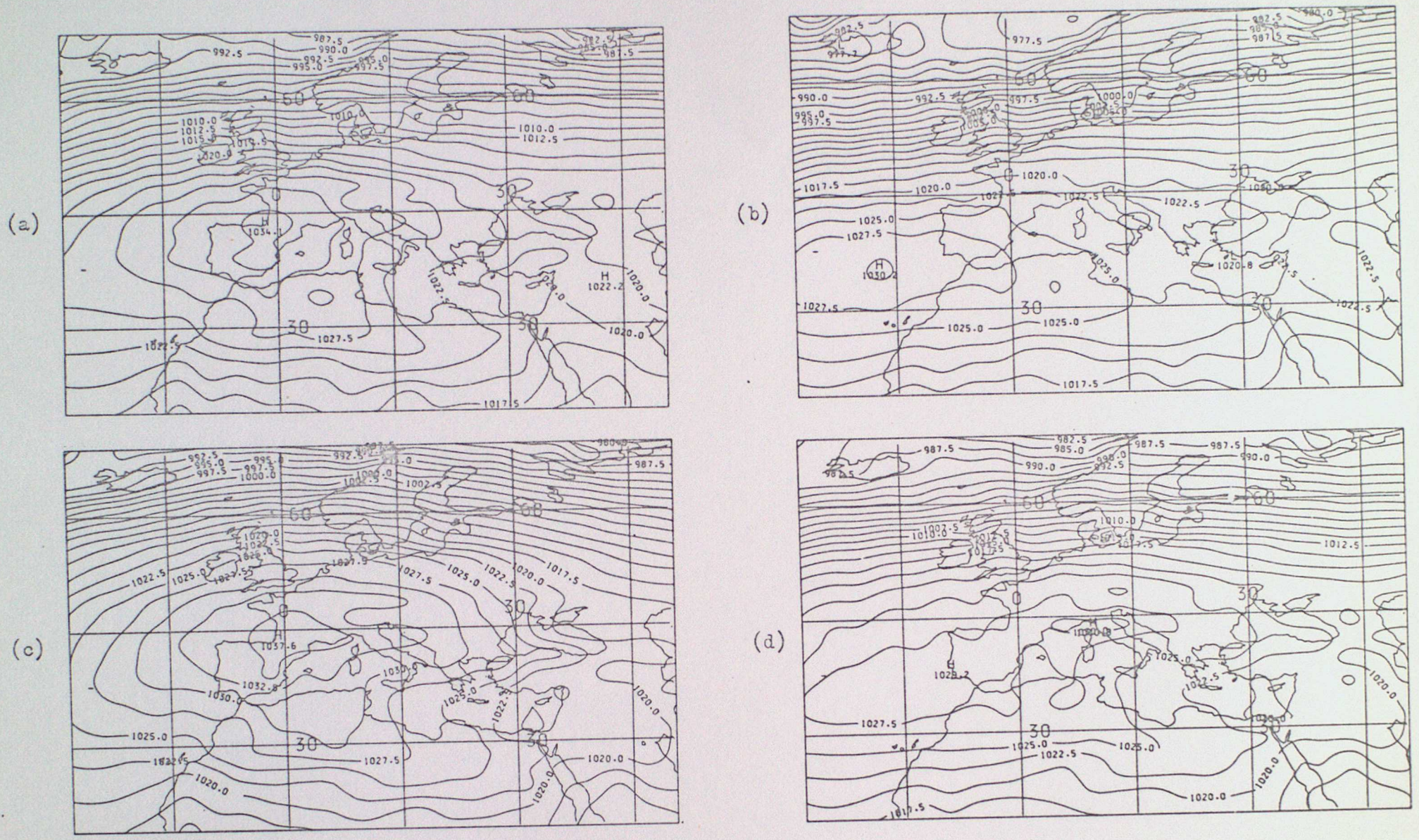

Figure 4 Model mean sea level pressure distributions for the Mediterranean region for (a) the first (b) the third (c) the fourth and (d) the fifth Januaries of the multiannual cycle integration. Contours are drawn at 2.5 mb intervals.

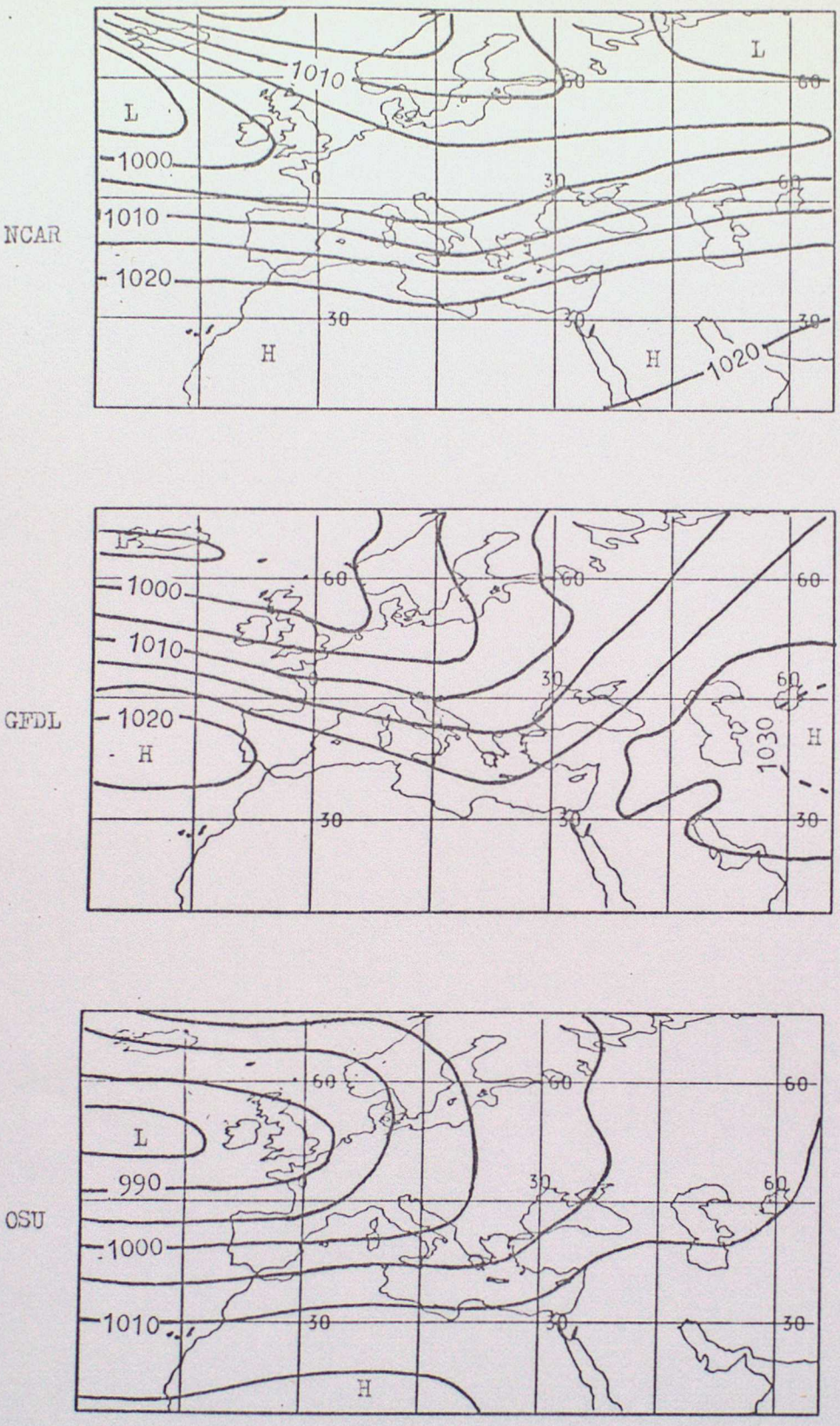

Figure 5 January simulations of mean sea level pressure for the third generation NCAR (Washington et al, 1979), 250 km resolution GFDL (Manabe et al, 1979) and OSU (Schlesinger and Gates, 1979) general circulation models. The contour interval used here is 5 mb.

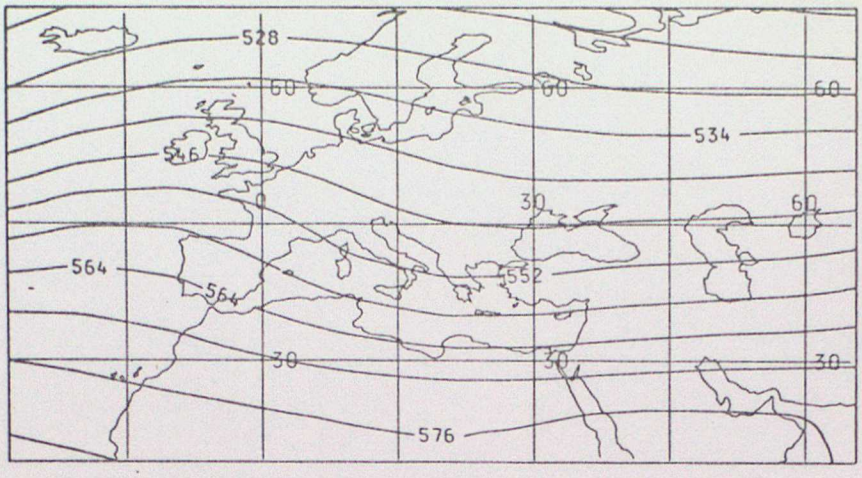

(a)

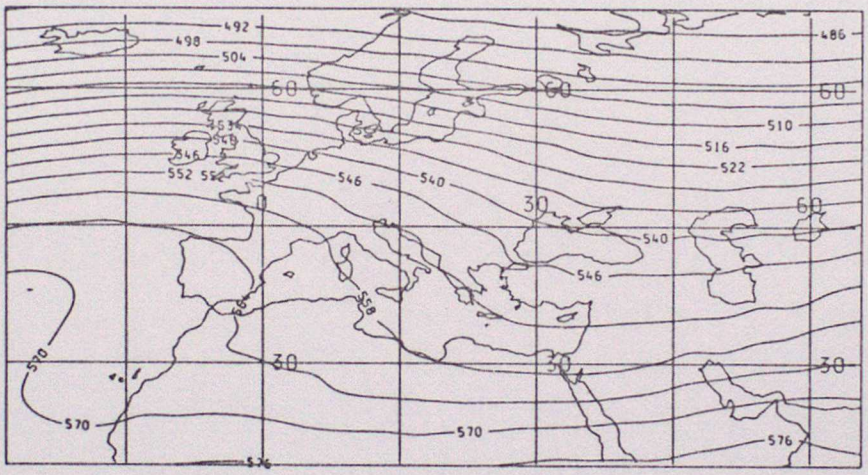

(b)

Figure 6 Comparison of (a) the observed climatological field of 500 mb heights for January (from Benwell, 1982) with (b) the model 500 mb height field for the second January of the multiannual cycle integration. The contour interval is 6 dagpm.

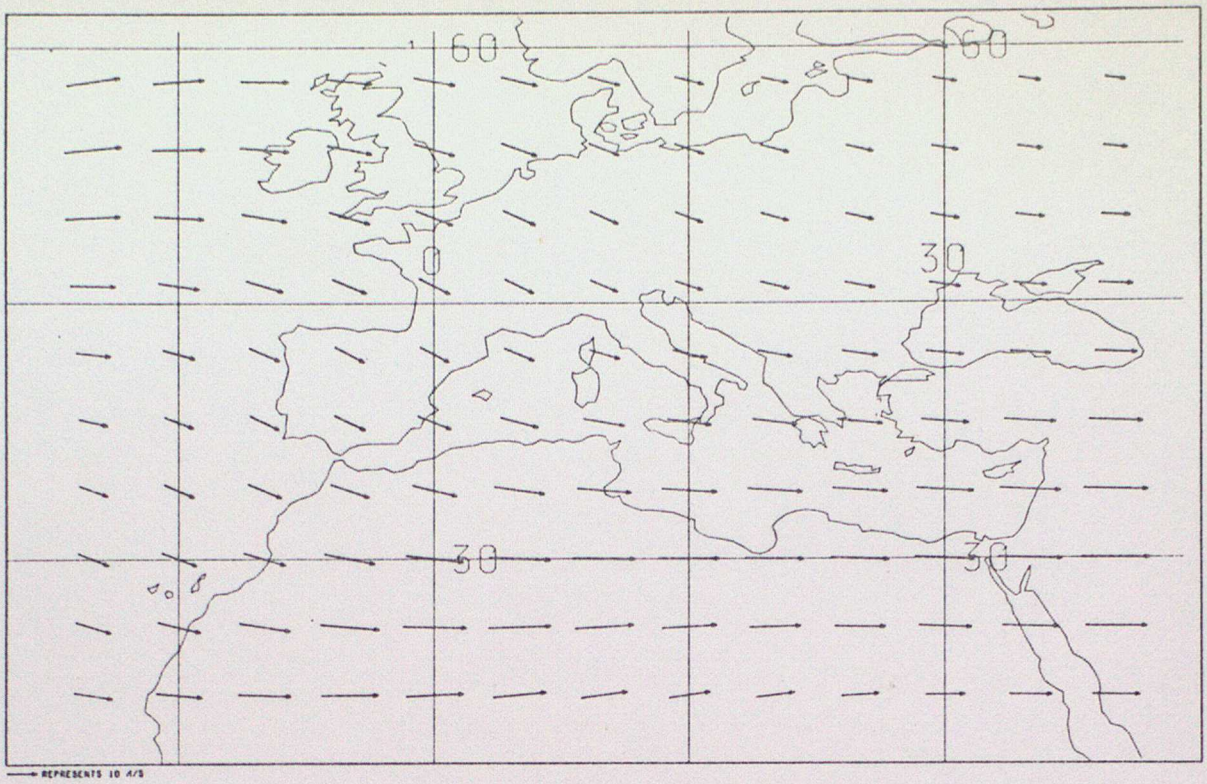

(a)

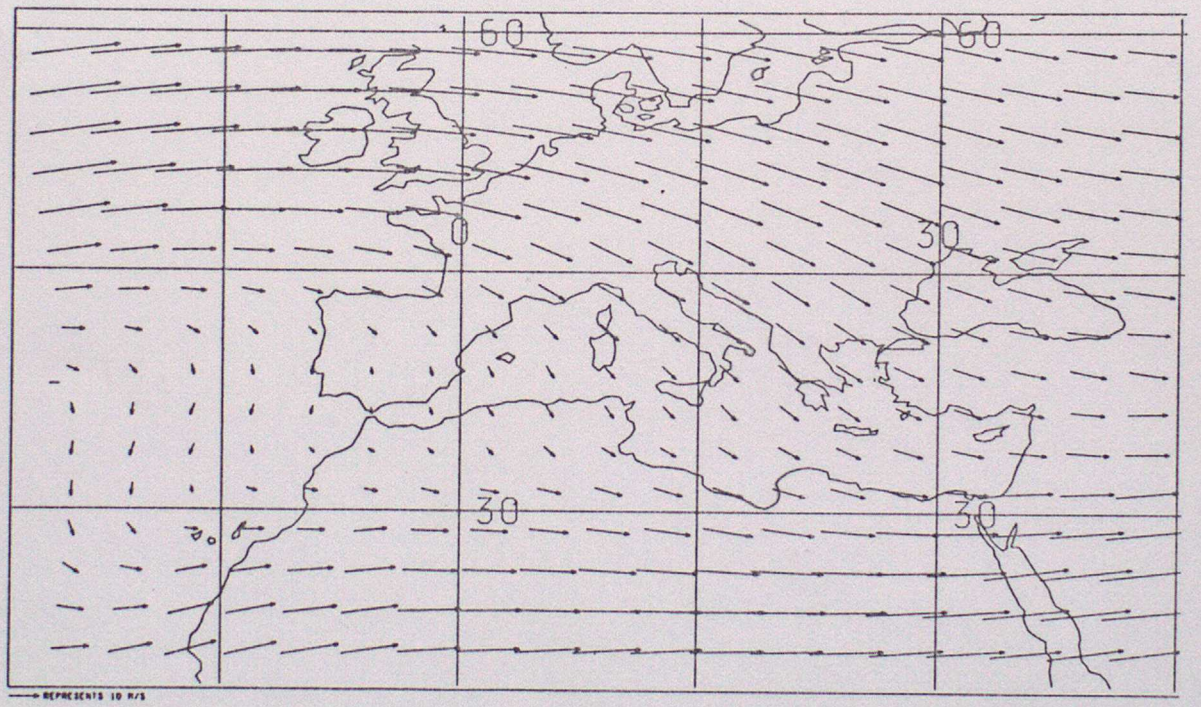

(b)

Figure 7 Comparison of (a) the climatological mean wind field at 400 mb averaged for the months of December, January and February (from Schutz and Gates, 1971) with (b) the corresponding model average wind field at 450 mb for the second winter of the multiannual cycle integration. The arrow to the bottom left of each chart represents a wind of 10 ms^{-1}.

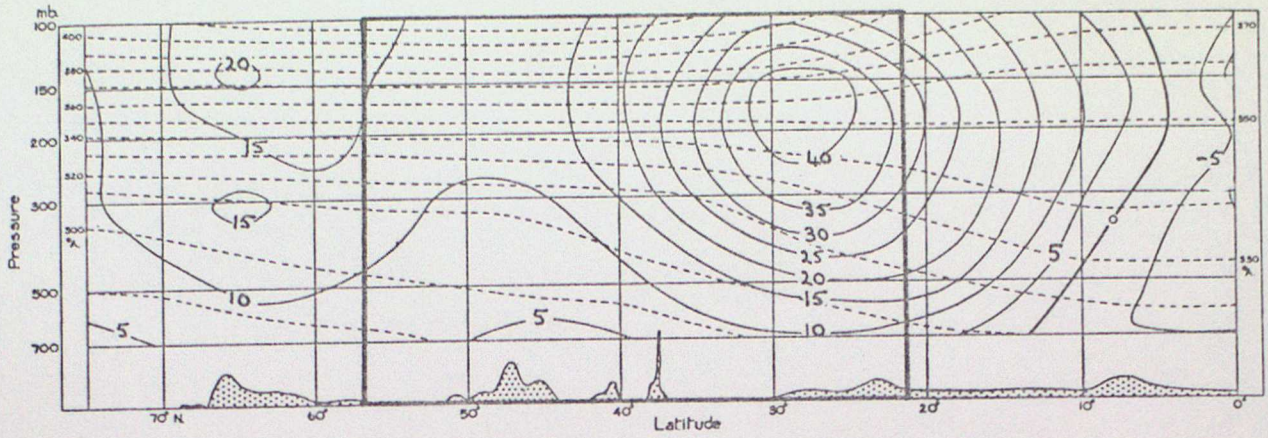

(a)

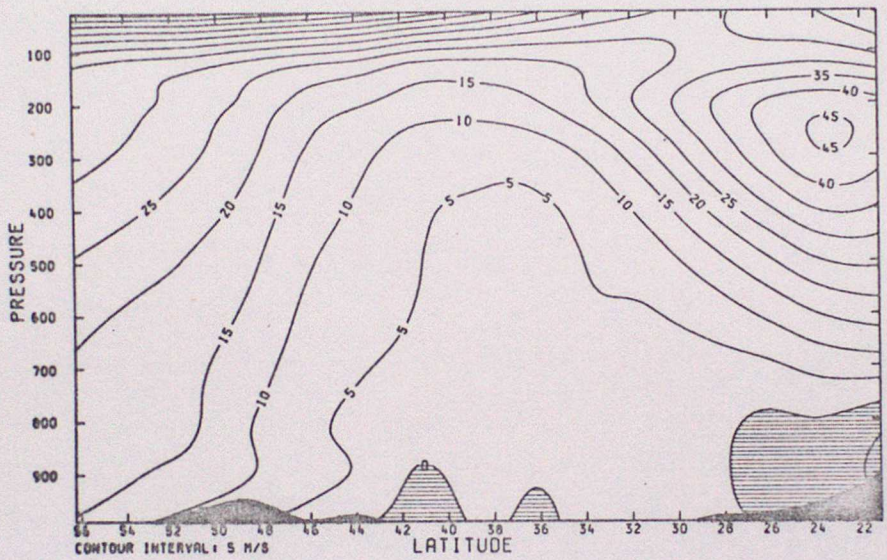

(b)

Figure 8 (a) Cross section at 15°E showing wind speeds (and potential temperatures) for January (from Meteorological Office, 1962). An easterly wind is indicated by a negative value. (Pecked lines are isopleths of potential temperature).

(b) Mean east-west component of the wind at 17°E from the model for the second January of the multiannual cycle integration. Easterlies are shown hatched.

In each case the contour interval for wind is 5 ms^{-1}. The heavy line on (a) borders the area of the cross section covered by (b).

(a)

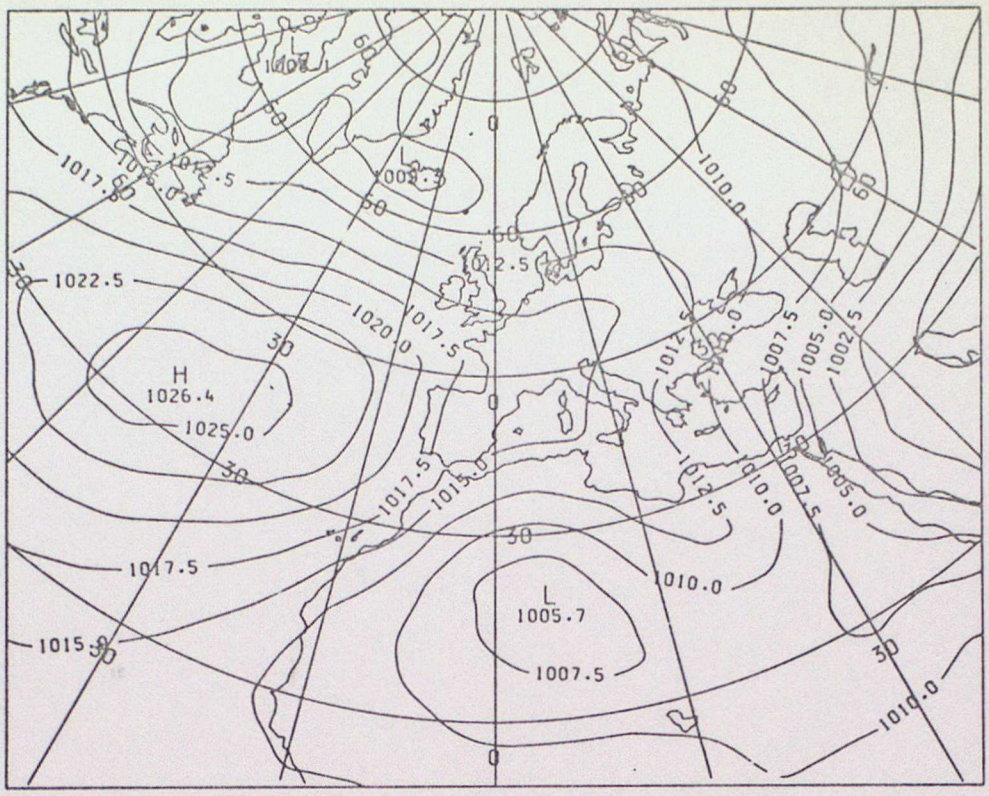

(b)

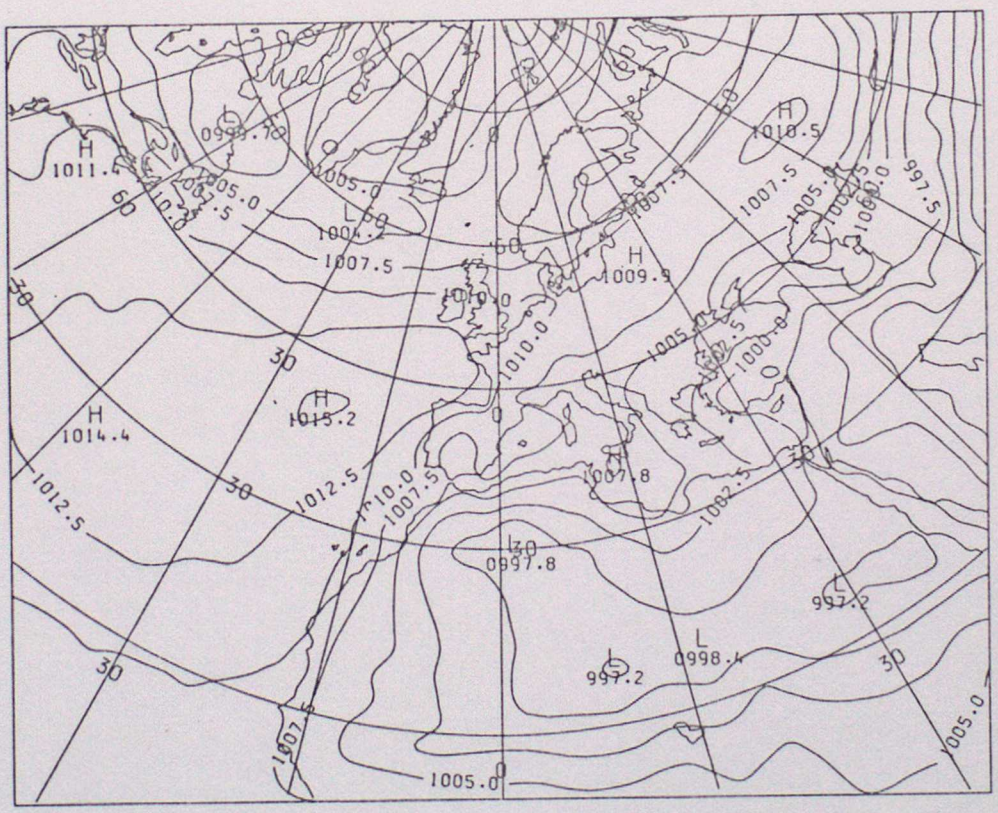

Figure 9 Comparison of (a) the observed climatological mean sea level pressure distribution for July for the Mediterranean and surrounding regions (from Schutz and Gates, 1972) with (b) the model mean sea level pressure distribution for the second complete July of the multiannual cycle integration. Contours are drawn at 2.5 mb intervals. Because of roundoff errors (see text) the model fields should be increased by some 6 mb everywhere for comparison with (a).

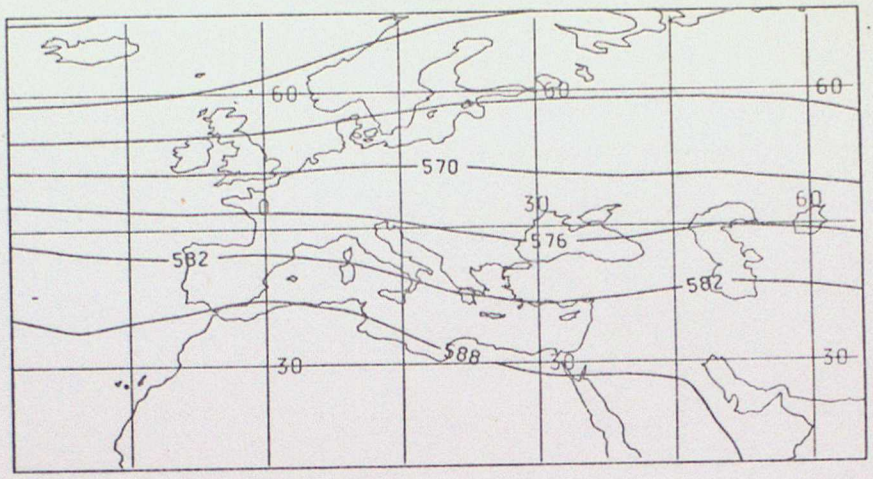

(a)

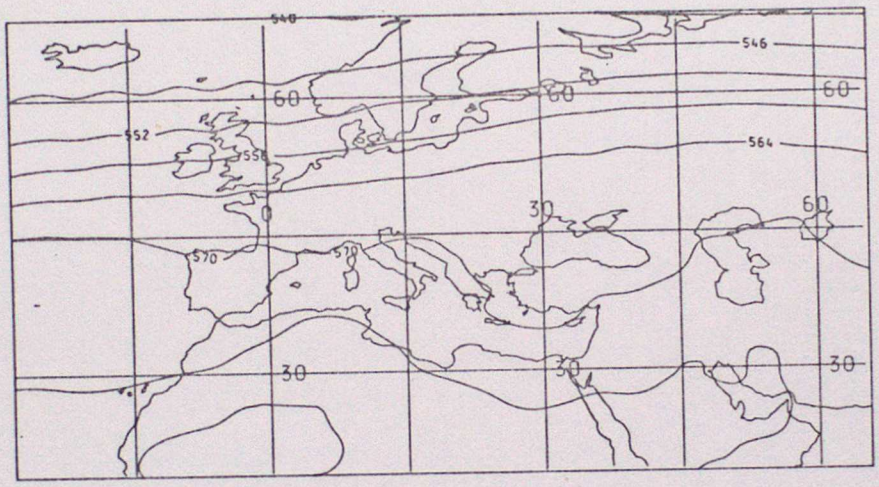

(b)

Figure 10 Comparison of (a) the observed climatological field of 500 mb heights for July (from Benwell, 1982) with (b) the model 500 mb height field for the second complete July of the multiannual cycle integration. The contour interval is 6 dagpm.

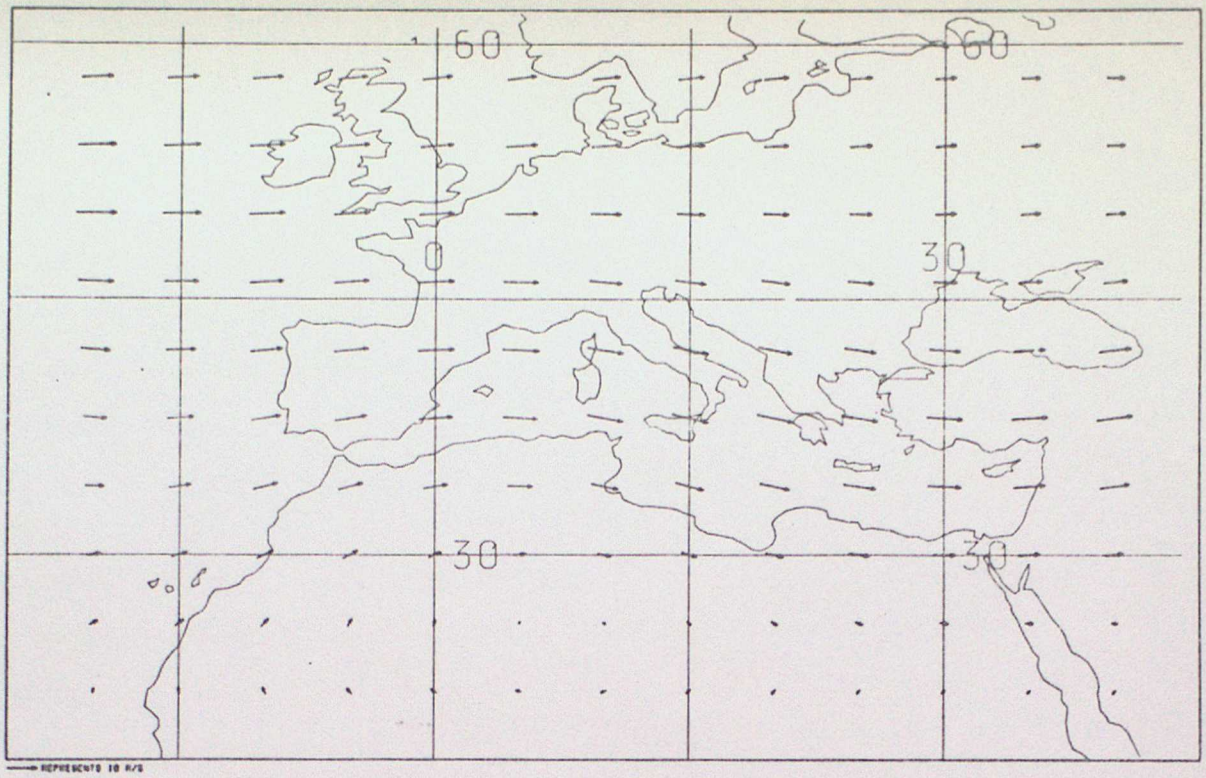

(a)

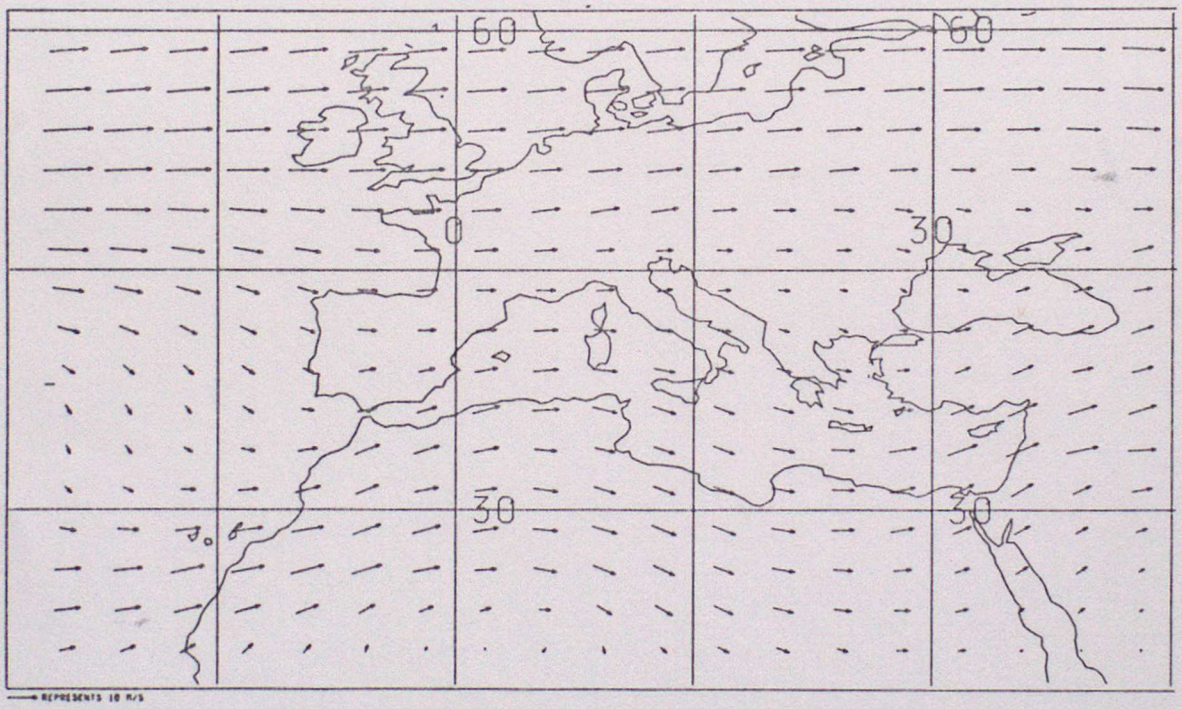

(b)

Figure 11 Comparison of (a) the climatological mean wind field at 400 mb averaged for the months of June, July and August (from Schutz and Gates, 1972) with (b) the corresponding model average wind field at 450 mb for the second complete summer of the multiannual cycle integration. The arrow to the bottom left of each chart represents 10 ms^{-1}.

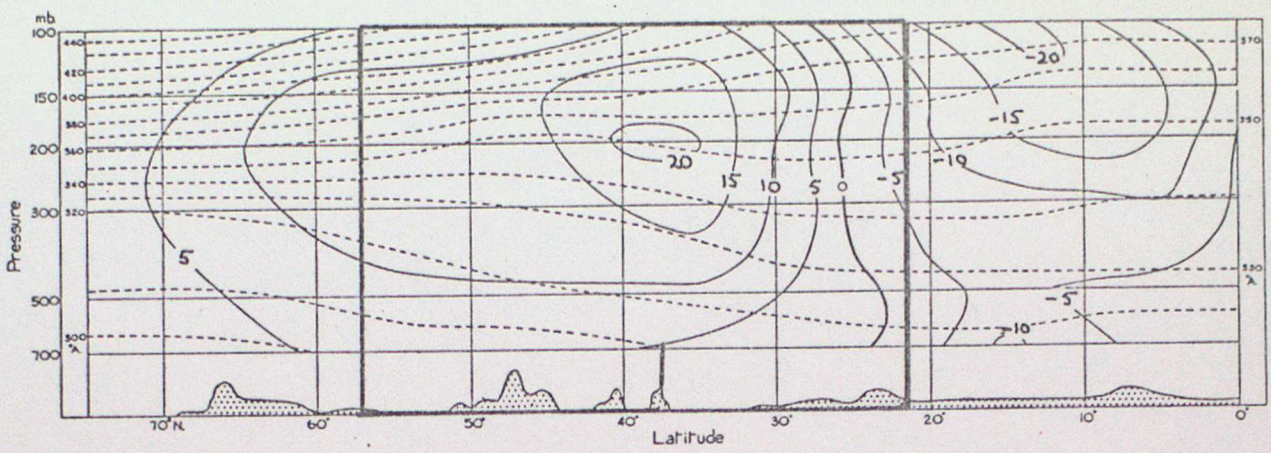

(a)

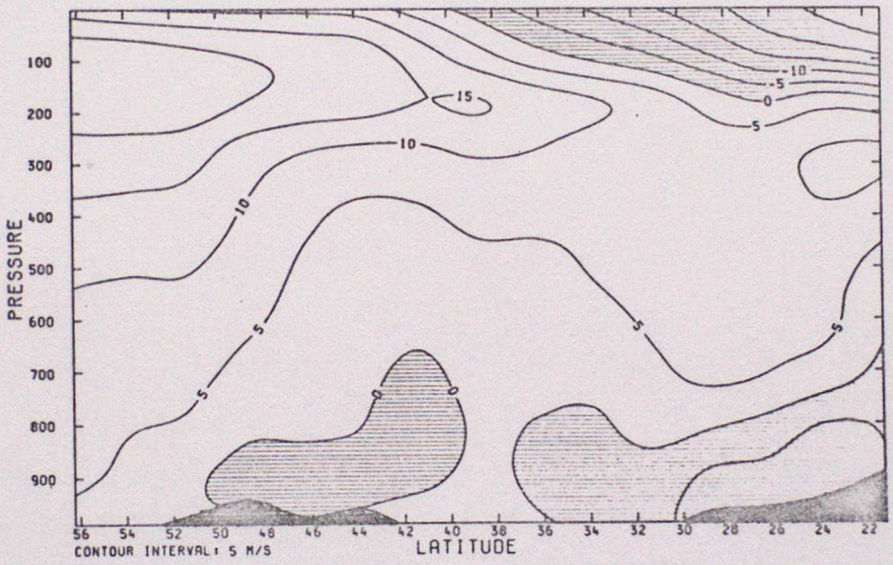

(b)

Figure 12 (a) Cross section at 15°E showing wind speeds (and potential temperature) for July (from Meteorological Office, 1962). An easterly wind is indicated by a negative value (pecked lines are isopleths of potential temperature).

(b) Mean east-west component of the wind at 17°E from the model for the second complete July of the multiannual cycle integration. Easterlies are shown hatched.

In each case the contour interval for wind is 5 ms^{-1}. The heavy line on (a) borders the area of the cross section covered by (b).

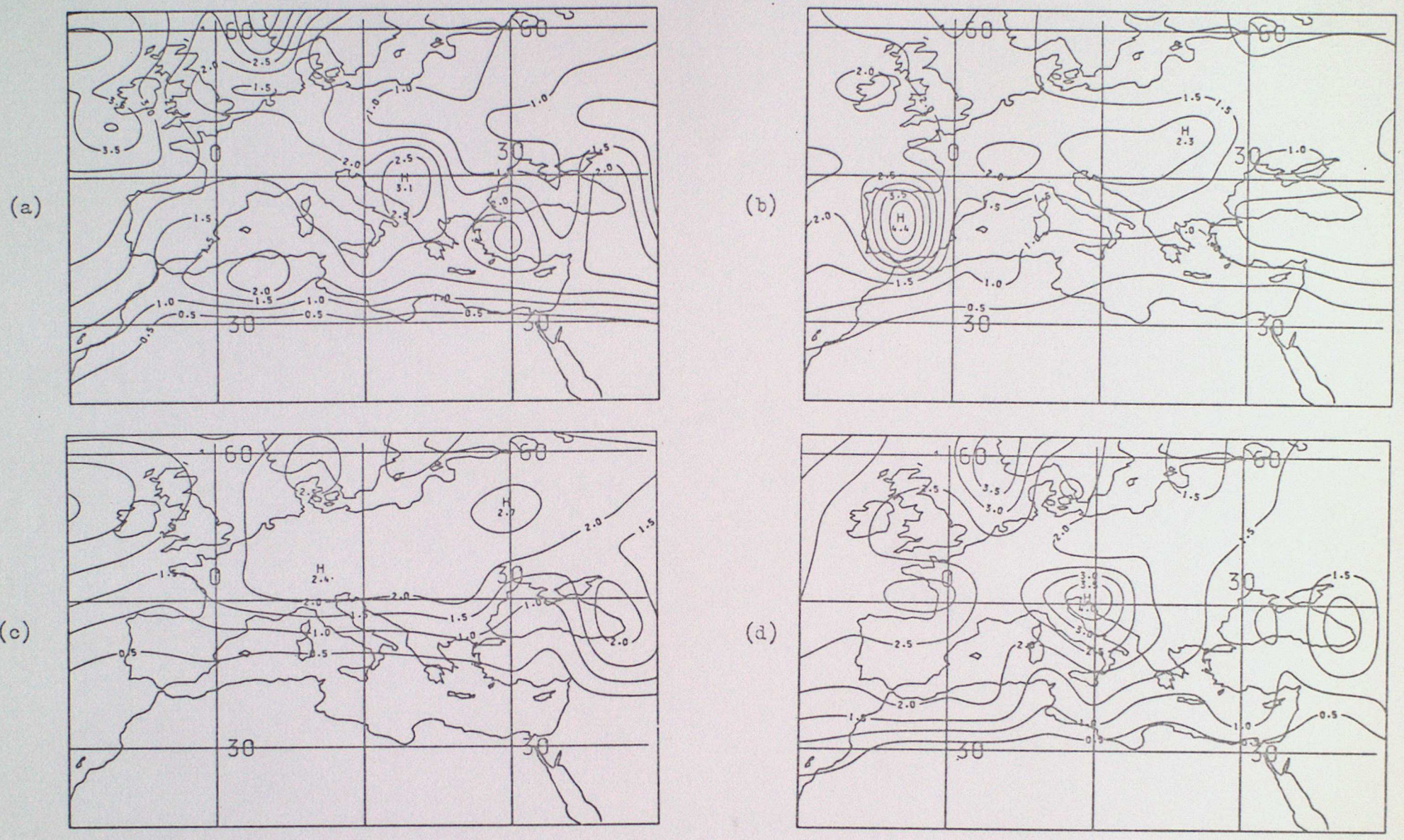

Figure 13 Observed climatological mean rainfall distribution over the Mediterranean region (from Schutz and Gates, 1971, 1972, 1973, 1974) for (a) winter (December, January, February), (b) Spring (March, April, May) (c) Summer (June, July, August) (d) Autumn (September, October, November). Isohyets are drawn at intervals of 0.5 mm day^{-1}.

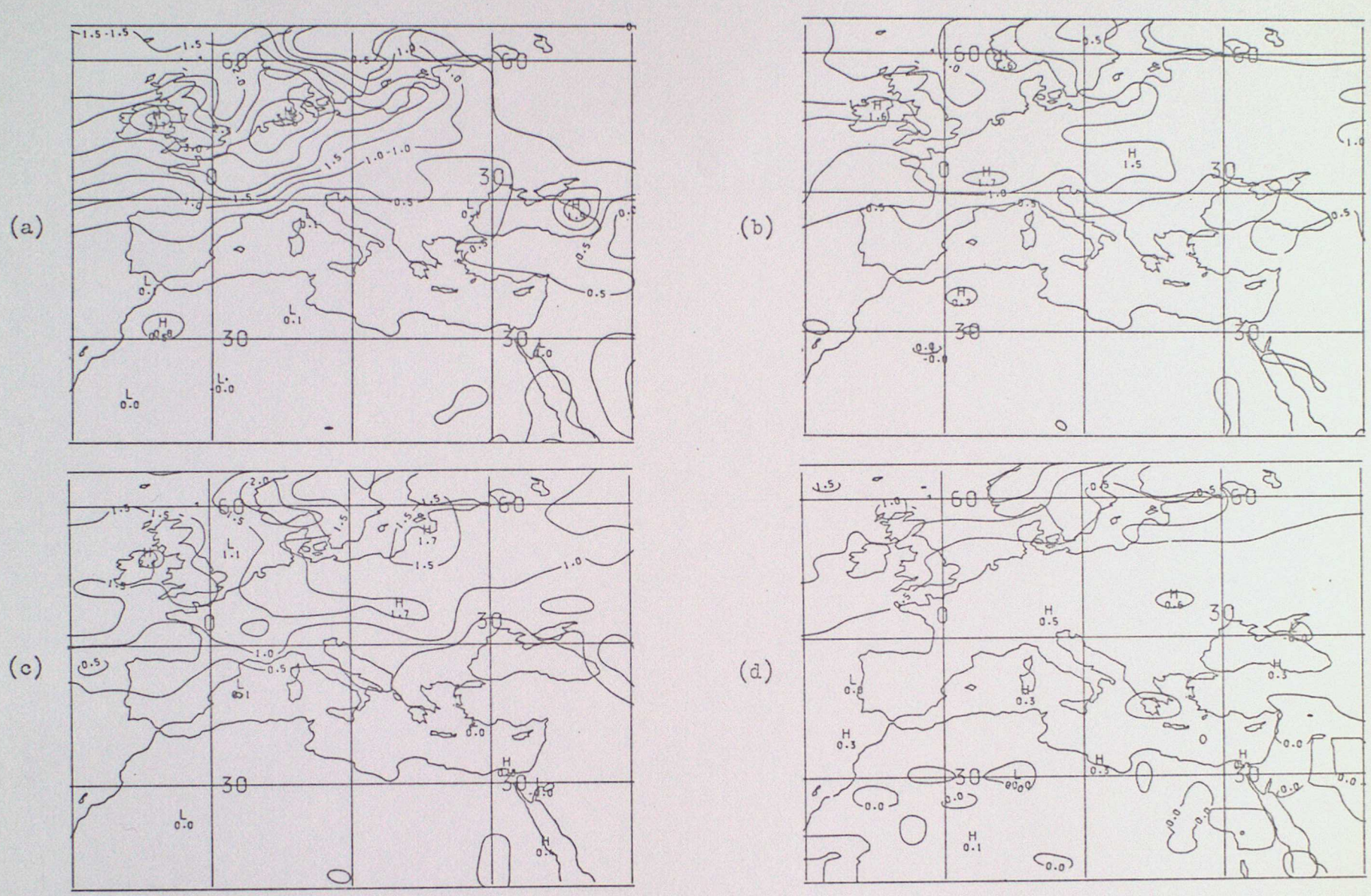

Figure 14 Model rainfall for the Mediterranean region resulting from condensation on the grid scale and averaged over (a) the second winter (December, January, February) (b) the second spring (March, April, May) (c) the second complete summer (June, July, August) and (d) the third autumn (September, October, November) of the multiannual cycle integration. Isohyets are drawn at intervals of 0.5 mm day^{-1}.

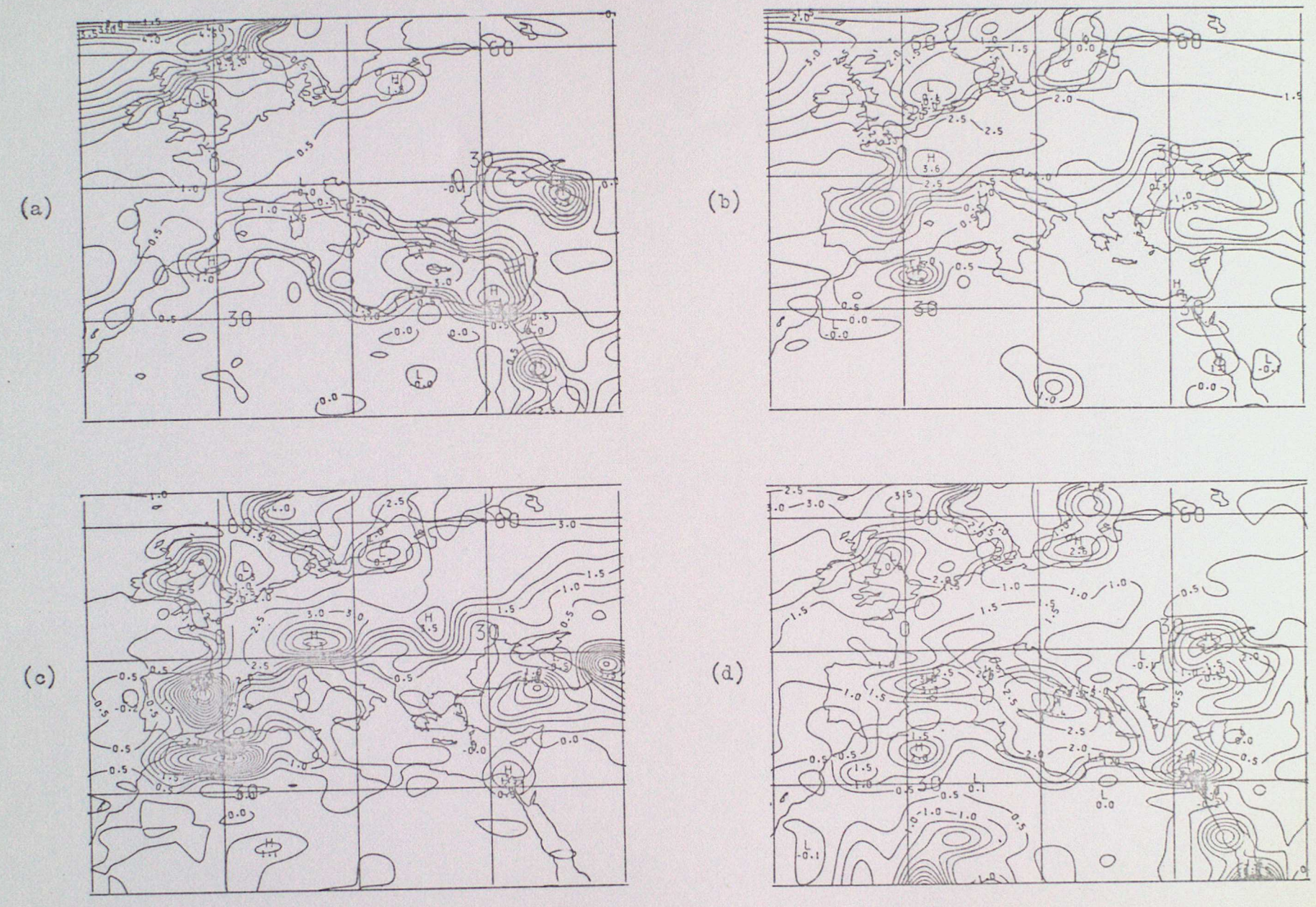

Figure 15 As Figure 14 but for model convective rainfall.

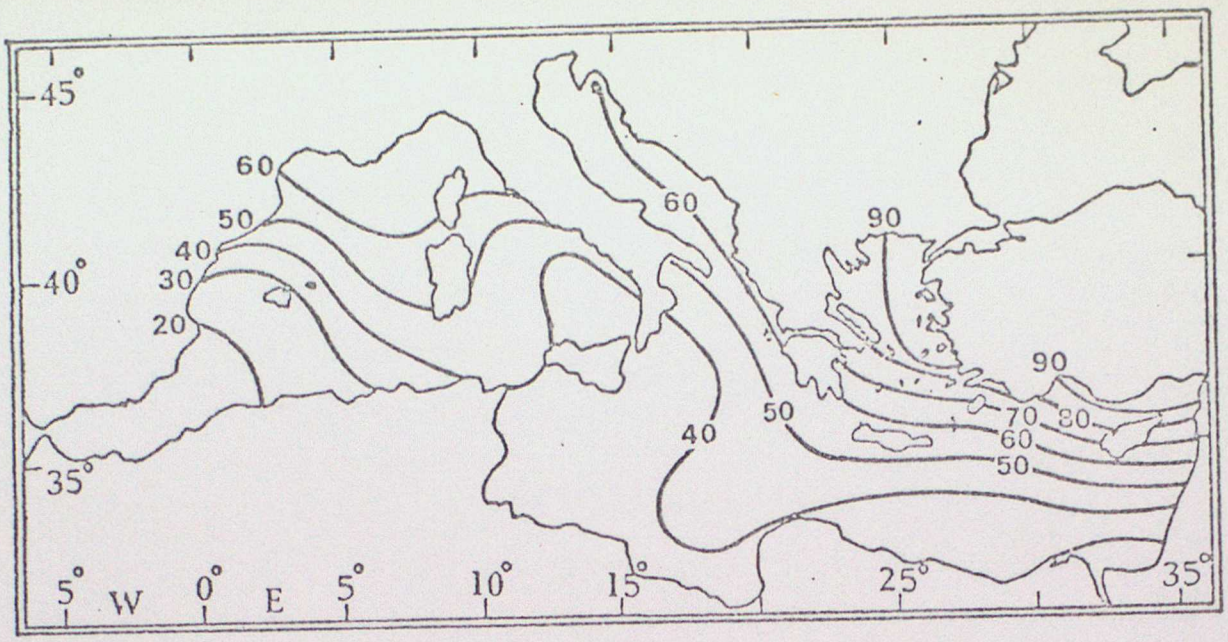

(a)

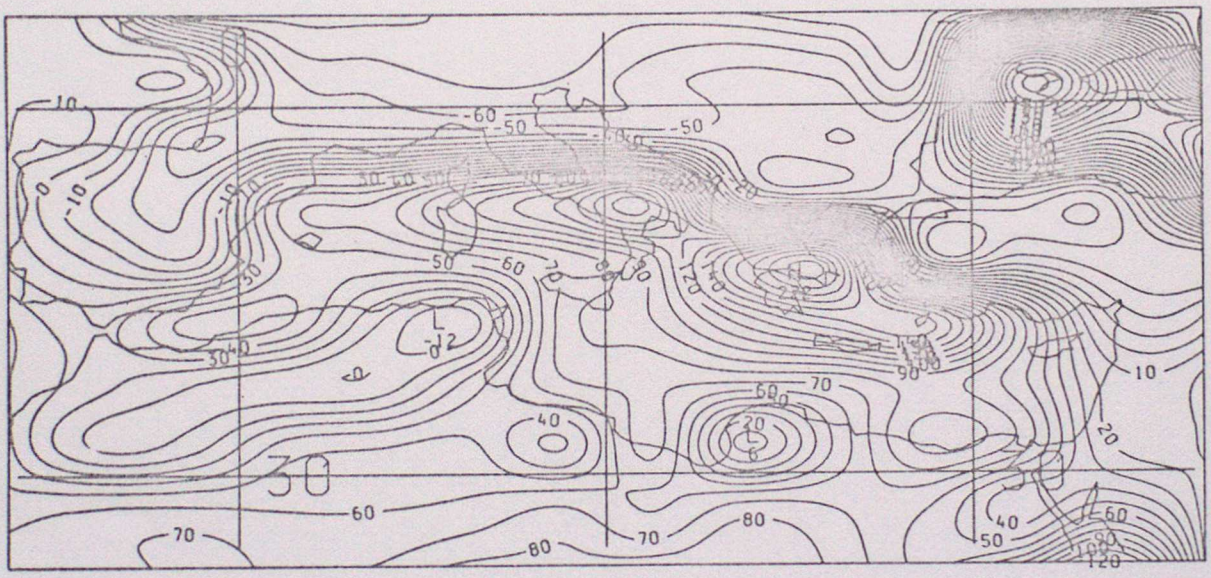

(b)

Figure 16 Monthly mean sensible heat flux from the surface to the atmosphere for January (a) as derived from observations by Repapis, Metaxis and Zerefos, 1978 and (b) from the model for the second January of the multiannual cycle integration. Contours are at intervals of 10 cal cm^{-2} day^{-1} (1 cal cm^{-2} day^{-1} = 0.48 Wm^{-2}).

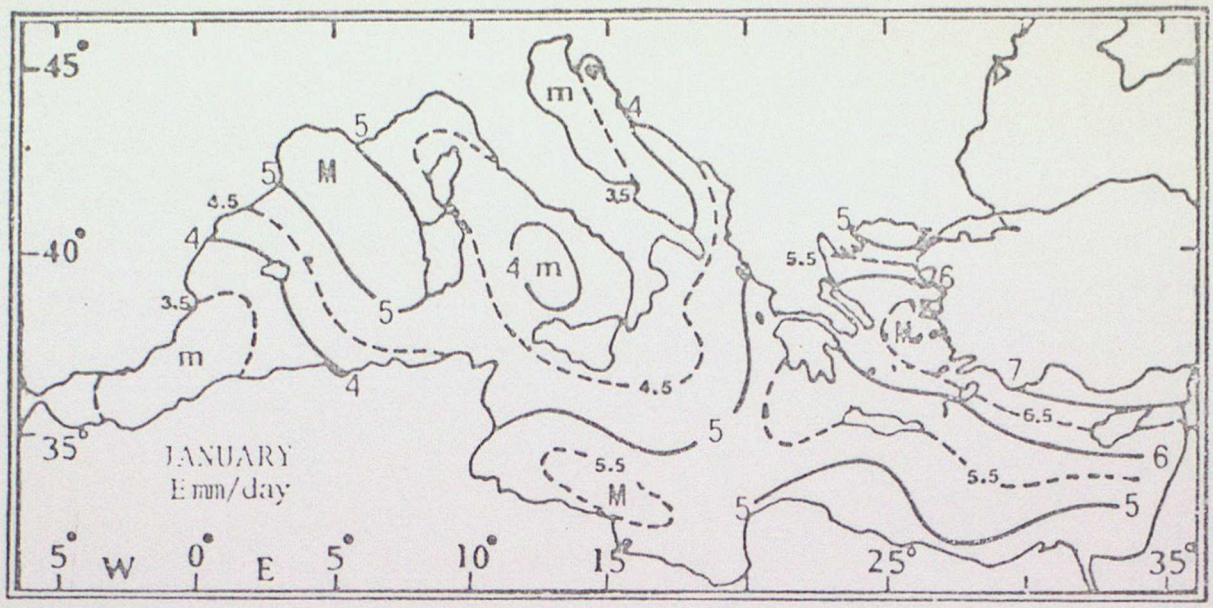

(a)

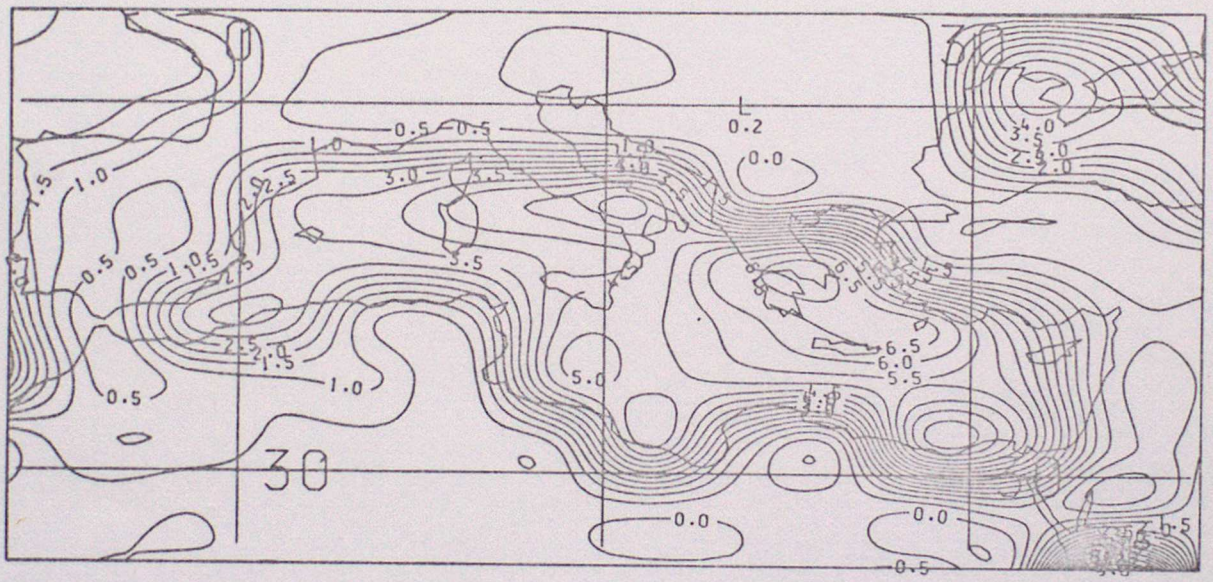

(b)

Figure 17 Monthly mean evaporation from the sea surface over the Mediterranean for January (a) as dervied by Metaxis and Repapis (1977) and (b) from the model for the second January of the multiannual cycle integration. Contours are at intervals of 0.5 mm day^{-1}.